REPORT DOCUMENTATION PAGE

Form Approved OMB No. 0704-0188

1. AGENCY USE ONLY (Leave blank)	2. REPORT DATE	3. REPORT TYPE AND DATES COVERED
	2000	Final Report

4. TITLE AND SUBTITLE

Laser with Wavelength 589 nm - Sodium Wavelength Laser

5. FUNDING NUMBERS

F61775-99-WE

6. AUTHOR(S)

Prof Nikolay Ilichev

7. PERFORMING ORGANIZATION NAME(S) AND ADDRESS(ES)

General Physics Institute
38 Vavilov St
Moscow 117942
Russia

8. PERFORMING ORGANIZATION REPORT NUMBER

N/A

9. SPONSORING/MONITORING AGENCY NAME(S) AND ADDRESS(ES)

EOARD
PSC 802 BOX 14
FPO 09499-0200

10. SPONSORING/MONITORING AGENCY REPORT NUMBER

SPC 99-4039

11. SUPPLEMENTARY NOTES

12a. DISTRIBUTION/AVAILABILITY STATEMENT

Approved for public release; distribution is unlimited.

12b. DISTRIBUTION CODE

A

13. ABSTRACT (Maximum 200 words)

This report results from a contract tasking General Physics Institute as follows: The contractor will develop a laser system based on F2 color centers in LiF crystals with frequency doubling to produce from 10 to 40W of average output power at 589 nm.

14. SUBJECT TERMS

EOARD, Adaptive Optics, Solid state lasers, Sodium wavelength laser

15. NUMBER OF PAGES

21

16. PRICE CODE

N/A

17. SECURITY CLASSIFICATION OF REPORT	18. SECURITY CLASSIFICATION OF THIS PAGE	19. SECURITY CLASSIFICATION OF ABSTRACT	20. LIMITATION OF ABSTRACT
UNCLASSIFIED	UNCLASSIFIED	UNCLASSIFIED	UL

Contract F61775-99-WE039

Laser with Wavelength 0.589 μm ("Sodium Wavelength Laser")

Final Report

Nikolay Il'ichev, General Physics Institute, Moscow, Russia

Summary

Continuous wave operation of a LiF: F_2^- laser with rotating active element with output power 270 mW at pump power 9 W at wavelength of generation 1.15 μm was obtained.

Theoretically investigated spectral characteristics of a Fabry-Perot interferometer with grating as one of its mirror. It was shown that implementation of this interferometer as output mirror of a tuned LiF:F_2^- laser gives a possibility to obtain narrow width (less than 0.1 cm^{-1}) spectrum of the laser radiation.

Suggested scheme of spectral selection was tested experimentally and spectral width of radiation less than 0.1 cm^{-1} was obtained. Frequency stability of radiation was better than 0.1cm^{-1} during 20 minutes of lasing. This experimental data show that the scheme of spectral selection is workable in principal.

Future Directions

Possible ways for further improvement of the LiF:F_2^- laser performance.

1. Perfection of the spectral selection scheme.

   1.1. Optimisation of its mirror reflectivity from the point of view of the laser efficiency and spectral selectivity;

   1.2. Experimental determination of parameters of the spectral selection elements (telescope, grating, and optical wedges) to obtain needed spectral purity of the laser radiation;

   1.3. Development of electronic and optical parts of the scheme to monitor wavelength of radiation;

   1.4. Development of stable mechanical construction of the laser.

2. Raising of output power of the LiF:F_2^- laser.

   To have higher output power in our construction it is necessary to raise the pump power. Estimations show that in our construction at 100 – 200 W pumping power (at wavelength 1.064 μm, and with divergence close to diffraction limited) it is possible to obtain output power 20 – 50 W.

3. Implementation of laser diodes as pump source for the LiF:F_2^- laser.

   Choosing of pumping radiation wavelength at peak of absorption F_2^- cc gives the possibility to have length of the LiF crystal smaller at the same concentration of the cc, and to have lower level of passive losses at wavelength of generation which in turn leads to higher efficiency of laser generation.

Contents

1. Development of a rotating LiF active element construction.

2. Generation characteristics of a cw LiF:F_2^- laser with rotating active element.

3. Theoretical study of ways to obtain and stabilise frequency of LiF:F_2^- - laser.

4. Continuous wave LiF:F_2^- cc laser with narrow spectrum width.

5. Future Directions.

6. Conclusion

1. Development of a rotating LiF active element construction.

To obtain high power (50 – 100 W) output radiation from LiF:F_2^- cc laser at laser pumping it is necessary to find technical solution of heat removing from LiF active element (AE). It was suggested earlier [1, 2] that rotation of AE is possible solution of the problem.

Important requirement to construction of rotating AE is that the LiF rotation should not misalign the laser resonator. There are two main causes of misalignment due to LiF rotation: a) optical wedge in the active element, and b) possible angle between perpendicular to optical surface of LiF and axis of rotation. The a) cause can be solved at a stage of manufacturing of the LiF and b) can be solved by an appropriate construction of LiF holder.

In Fig. 1 there is draft of the LiF active element, which was implemented in LiF:F_2^- - laser. Pure LiF (without colour centres) was used at the stage of manufacturing. Colour centres in polished LiF were done by γ - irradiation of the crystal. Our crystal had initial transmission at wavelength 1.064 μm- 50 % and transmission at wavelength 1.18 μm - 86 %, crystal length was 28 mm. The crystal was not AR coated.

In Fig. 2 there is layout of mechanical parts of LiF rotation scheme. Steel axis is resting and all other parts are rotating in two ball-bearings. Three screws aligned attitude of the perpendicular to optical surfaces of the LiF with respect to axis of rotation as it is shown in Fig. 2. Sheet rubber gave needed flexibility for it (see Fig. 2).

In Fig. 3 there is kinematic scheme of LiF rotation.

2. Generation characteristics of a LiF: F_2^- laser with rotating AE.

The cw LiF:F_2^- laser with rotating active element was put into operation at pumping by cw YAG:Nd laser. Construction of a rotating LiF:F_2^- active element mount is described above. The LiF crystal had initial transmission at wavelength 1.064 μm 50 % and transmission at wavelength 1.18 μm - 86 %, crystal length was 28 mm. The crystal was not AR coated. Scheme of the colour centre laser resonator is presented in Fig. 4. 1 and 4 are the resonator mirrors. Parameters of the mirrors are: 1 - radius of curvature 6.5 cm, reflectivity at 1.15 –1.19 μm is 99%, transmission at wavelength 1.064 μm is 70%, 2 - radius of curvature 500 cm, reflectivity at 1.15 μm is 95%, reflectivity at wavelength 1.064 μm is about 95%. Pump radiation passed through mirror 1 and illuminated LiF:F_2^- the crystal 2. There is a lens 3 inside the resonator. Focal length of the lens is 20 cm. The resonator length is 250 cm, distance between mirror 1 and lens is 27.5 cm. Resonator scheme was chosen in a such a way that the resonator parameters would be not sensitive to the focal length of a thermal lens inside the LiF, which is due to heating of the active element under pump radiation. There is calculated TEM_{00} – mode diameter

near the middle of the active element as function of co-ordinate along optical axis of the resonator for different focal lengths of the lens in Fig. 5. One can see that mode diameter depends on focal length of lens weakly if lens force is less than $\left|\frac{1}{f}\right| \le 20$ diopters.

There is experimental dependence of output power of the cw LiF:F_2^- - laser with rotating active element as function of input power in Fig. 6. Input power was measured at input face of the LiF:F_2^- - crystal. Pumping laser was a cw YAG:Nd laser with output power about 20 W. Only half of this power was available for pumping of the LiF:F_2^- - crystal because transmission of mirror 1 (see Fig. 4) at 1.064 μm was 70 % and matching lenses (are not shown in Fig. 4) were not AR coated. Rotation frequency was 2 – 3 Hz. Pump power threshold was 4.2 W, slope efficiency 5.7%. Output power 270 mW was obtained at pump power 9 W. Wavelength of generation was 1.15 μm. Outer surface of the active element was cooled by evaporating of alcohol from the surface. If rotation of the active element is stopped then the laser oscillation is ceased during time less than one second. LiF:F_2^- - laser generation at pumping by chopped cw YAG:Nd laser was reported in [3]. Authors of this work observed ceasing of generation if pumping beam was not chopped and beginning of generation if at this time the LiF crystal was moved. Quenching of generation in [3] was explained by thermooptical distortions of the laser resonator due to heating of the LiF crystal under pump radiation. Here we report the first observation of high power cw LiF:F_2^- - laser generation.

3. Theoretical study of ways to obtain and stabilise frequency of LiF:F_2^- - laser.

This part of the present report is concerned with theoretical study of spectral selection in a LiF:F_2^- laser. The aim is the suggestion of particular technical solution for the laser. Full revue of methods of spectral selection and frequency tuning exceeds the limits of our consideration. This is the reason why some methods of spectral selection (anisotropic filters for example) are not discussed here.

By the technical requirements it is necessary to have 3 GHz at wavelength 0.589 μm after SHG process, which corresponds to about 1.5 GHz ($\Delta\nu$=0.05 cm^{-1}) at wavelength λ_0=1.178 μm ($\nu_0=1/\lambda_0$=8489 cm^{-1}). In [3] we obtained experimentally that spectral width of the laser generation was about 30 cm^{-1} with two glass prisms as spectral selection element. This value is far from needed but it is useful because it forms some requirements to spectral selection element. Fabry-Perot interferometer (FPI) and grating are discussed below.

Fabry-Perot interferometer

There are two usual ways of implementation FPI. The first one is when FPI is output mirror of a laser and the second one is when FPI is placed inside a laser resonator and frequency dependent losses are due to frequency dependent transmission of a FPI. In the last case the interferometer should be inclined with respect to resonator optical axis so that reflected beam goes out from the resonator. In the first method FPI has two functions simultaneously: as output mirror and spectral selection element. These two functions have requirements that can in principle contradict each other. So we discuss here internal resonator FPI only. Transmission T of a FPI depends on reflectivity of its mirrors R_1 and R_2, and distance (interferometer base) between mirrors d

$$T = \frac{(1-R_1)\cdot(1-R_2)}{1+R_1\cdot R_2 - 2\cdot\sqrt{R_1\cdot R_2}\cdot\cos(2\cdot\varphi)}, \qquad (1)$$

where $\varphi = 2\cdot\pi\cdot\nu\cdot d\cdot\cos(\theta)$, $\nu = \frac{1}{\lambda}$, d – interferometer base, λ - wavelength of radiation, θ - angle between perpendicular to FPI mirrors and wave vector of the incident light. This expression for R_1=R_2 can be found in [4]. Let us estimate d and reflectivity of FPI mirrors R_1 and R_2 to have spectrum generation width 0.05 – 0.1 cm^{-1}. The base of FPI should be at least d<1/2$\Delta\nu_g$=100 μm at $\Delta\nu_g$=50 cm^{-1} because width of a LiF:F_2^- laser generation spectrum is 30 cm^{-1} (see above) and frequency separation of orders of interference should be more than this value with some margin of safety. Let us estimate FPI parameters requirements specifications. If d=94.24 μm, R_1=R_2=90% then from (1) it is easy to obtain frequency width of FPI transmission per two passes: FWHM=1.14 cm^{-1}. For rough estimation of generation spectrum width one can take 10 double passes of radiation through FPI. This gives us 0.3 cm^{-1}. For lower reflectivity of FPI mirrors FWHM is higher (for example FWHM=4 cm^{-1} at R_1=R_2=70%). Transmission of FPI at maximum depends on ratio between R_1 and R_2. If R_1=R_2 then T=100% and for R_1=89% and R_2=91% T=97.8%. This estimation shows that at high reflectivity of a FPI mirrors ($R \approx$90%) accuracy of mirrors reflectivity manufacturing becomes strict. So technically it is difficult to obtain spectrum width 0.05 – 0.1 cm^{-1} with the help only one FPI. With two or more FPI with different values of d it is possible to solve the problem but the new problem arises the problem of controlling of these interferometers bases. We suppose that the development of reliable spectrum selecting system on the base only internal resonator FPI is rather difficult task.

Grating as a spectral selector

It is known that implementation of internal resonator grating is the safe way to solve the problem (see for example [6, 7]). The main disadvantage is the high level of internal resonator losses due to reflection of radiation in different orders of diffraction. It should be mention here that the cw LiF:F_2^- laser is sensitive to internal resonator losses (see above). To overcome the

problem of high losses we suggest here to use as output mirror an interferometer Fabry-Perot with grating as one mirror (FPIG). In Fig. 7 there is a scheme of this interferometer: 1 is a mirror with reflectivity R_1, 2 is a grating with reflectivity R_2, 3 is an additional mirror with reflectivity R_3 to let a radiation go out from the interferometer. The grating works at autocollimation mode of operation and reflects an incident radiation at needed frequency back. It is possible to obtain expression for amplitude reflectivity r of this interferometer for plane wave

$$r = \frac{-r_1 + r_2 \cdot R_3 \cdot \exp(2 \cdot i \cdot \varphi)}{1 - r_1 \cdot r_2 \cdot R_3 \cdot \exp(2 \cdot i \cdot \varphi))}, \tag{2}$$

where r_1 and r_2 is amplitude reflectivity (relation between electric fields of reflected and incident waves) of mirror 1 and grating accordingly ($R_1=|r_1|^2$, $R_2=|r_2|^2$, $R=|r|^2$), d is distance between mirrors 1 and 2 along axis of FPIG. The distances from mirror 1 and opposite ends of the grating are different because the grating is inclined. We choose d as distance to the middle of the grating. This statement follows from the next expression (3) below. Amplitude reflectivity of a grating at autocollimation mode of operation for plane wave can be found with the help of expressions from [4] and [5]

$$r_2 = \sqrt{R_{20}} \cdot \frac{\sin(\pi \cdot \frac{\nu}{\nu_0} \cdot N \cdot m)}{N \cdot \sin(\pi \cdot \frac{\nu}{\nu_0} \cdot m)} \cdot \exp(i \cdot \pi \cdot \frac{\nu}{\nu_0} \cdot (N-1) \cdot m). \tag{3}$$

N is number of grooves of illuminated part of grating ($N=Lg$, L is length and g is number of grooves per unit of length), ν and ν_0 are frequency and working frequency of radiation, m is order of diffraction, R_{20} is reflectivity of grating at working order of diffraction. It is assumed that angle of incidence for all frequencies is θ_0; reflected radiation goes back; condition $2 \cdot \sin(\theta_0) \cdot 2 \cdot \pi \cdot \nu_0 \cdot a = 2 \cdot \pi \cdot m$ (a is period of grating) is fulfilled. At these conditions expression (3) presents reflectivity as function of frequency when reflected radiation at different frequencies goes in one direction (back). In Fig. 8 there is reflectivity at frequencies of maximum FPIG reflectivity. These frequencies correspond to orders of interference of the interferometer. Numeric parameters for calculation are the next: R_1=80%, R_{20}=60%, R_3=30%, L=5 cm, g=600 grooves/mm, m=1, d=250 cm. Exact value of d is not important until $d>>1/\Delta\nu$, $\Delta\nu$ is frequency width of the interferometer.

Output radiation intensity I_{out} is connected with input one I_{in} (see Fig. 7): $I_{out}=T_{out}I_{in}$. From (2) at frequencies where reflection coefficient of FPIG is maximum (R_{max}) one can find T_{out}

$$T_{out} = \frac{(1-R_1) \cdot (1-R_3)}{1 + R_1 \cdot R_2 \cdot R_3^2 + 2 \cdot \sqrt{R_1 \cdot R_2} \cdot R_3}. \tag{4}$$

FPIG possesses some losses that are immanent feature of the interferometer. One part of these losses is connected with reflection of light by grating into different orders. Other part is due to passing of radiation through mirror 3 (see Fig. 7) at some angle to output direction. For estimation of value of these losses let us present FPIG as a system with effective reflection coefficient R_{max} and passive filter, that is placed after this mirror. This model is useful for estimation of efficiency of a laser with FPIG as output mirror. Effective transmission T_{eff} of this filter is

$$T_{eff} = \frac{T_{out}}{1 - R_{\max}} \tag{5}$$

There is T_{eff} as function of frequency in Fig. 9. Parameters of FPIG are the same as for the curve in Fig. 8. One can see from Fig. 9 that transmission of this imaginary filter is 70 % – 74 % and only about 30 % are lost. This value is not high and after all we should to remember that threshold is higher when a grating is placed inside the resonator with usual output mirror instead of FPIG.

Frequency of LiF:F_2^- laser output radiation depends on not only frequency characteristics of the laser resonator. It depends on frequency characteristics of amplification and absorption coefficients of F_2^- colour centres in LiF too. It is possible that for some frequency threshold is lower than for working one. Let us calculate threshold of a LiF:F_2^- laser with frequency dependent losses in the frequency region where generation is possible. Let us denote $\sigma_a(\nu)$ and $\sigma_e(\nu)$ absorption and emission cross-sections of laser transition, N_1 and N_2 population density (number of particles per cm^3) of lower and upper laser states, $N_0=N_1+N_2$, N_0 is density of colour centres. For amplification coefficient we have

$\alpha(\nu) = \sigma_e(\nu) \cdot N_2 - \sigma_a(\nu) \cdot N_1 = (\sigma_e(\nu) + \sigma_a(\nu)) \cdot N_2 - \sigma_a(\nu) \cdot N_0$. Threshold condition is

$\alpha(\nu) \cdot 2 \cdot l = \chi(\nu)$, where $\chi(\nu)$ are internal resonator losses, l is a length of LiF active element (AE). Pump power threshold is proportional to N_2. From this and previous equation we find N_2:

$N_2(\nu) = \frac{1}{\sigma_e(\nu) + \sigma_a(\nu)} (\sigma_a(\nu) \cdot N_0 + \frac{\chi(\nu)}{2 \cdot l})$. Absorption coefficient at pump frequency ν_p is

$\alpha_{ab}(\nu_p) = \frac{1}{2 \cdot l} \ln(\frac{1}{T_p})$, T_p is initial transmission of AE. We can find N_0 from $\alpha_{ab}(\nu_p) = \sigma_a(\nu_p) \cdot N_0$.

Combining all these equations we find ratio of thresholds at frequency ν and at working frequency ν_0:

$$\gamma(\nu)=\frac{N_2(\nu)}{N_2(\nu_0)}=\frac{\sigma_e(\nu_0)+\sigma_a(\nu_0)}{\sigma_e(\nu)+\sigma_a(\nu)}\cdot\frac{\frac{\sigma_a(\nu)}{\sigma_a(\nu_p)}\cdot 2\cdot\ln(\frac{1}{T_p})+\chi(\nu)}{\frac{\sigma_a(\nu_0)}{\sigma_a(\nu_p)}\cdot 2\cdot\ln(\frac{1}{T_p})+\chi(\nu_0)}. \qquad (6)$$

We estimate cross sections with the help of data from [8] $\sigma_a(\nu)=\sigma_{am}\cdot\exp(-\left(\frac{\nu-\nu_a}{\Delta_a}\right)^2)$,

$\sigma_e(\nu)=\sigma_{em}\cdot\exp(-\left(\frac{\nu-\nu_e}{\Delta_e}\right)^2)$, where Δ_a=825 cm^{-1}, Δ_e=800 cm^{-1}, σ_{am}=7.9·10^{-17} cm^2, σ_{am}=7.7·10^{-17} cm^2, ν_e=8850 cm^{-1} (λ_e=1.13 μm), ν_a=10417 cm^{-1} , (λ_a=0.96 μm).

In Fig. 10 (*a*) there is relative threshold of a LiF:F_2^- laser as function of wavelength with FPIG as output mirror, calculated with help of (6) at wavelength in the range 1.1 – 1.2 μm. Grating of FPI is aligned at wavelength λ_0=1.178 μm and parameters of FPIG are presented above, initial transmission of LiF:F_2^- at wavelength λ_p=1.06 μm is T_p=50 %. From Fig. 10 (*a*) one can see that at wavelength close to 1.15 μm threshold is only 8 % higher than at 1.178 μm. This is not safe because if pump power is not stable transient phenomena may occur and at some conditions generation close at 1.15 μm wavelength becomes possible. Some additional selector is necessary to change this situation. For example additional interferometer Fabry-Perot with short base *d* may be placed inside this laser resonator (between FPIG and rear mirror of the resonator). Total internal resonator losses in this case can be found with the help of expression

$$\chi(\nu)=\chi 0+\ln(\frac{1}{R})+2\cdot\ln(\frac{1}{T}), \qquad (7)$$

where R is found from (2) ($R=|r|^2$) at frequencies where reflectivity is maximum, T is found from (1) at frequencies where transmission is maximum, χ_0 presents summarised losses due to passive absorption in LiF AE, diffraction losses and so on. Result of calculation is shown in Fig. 10. Parameters of additional FPI are: d=5.981 μm ($d\cdot\cos(\theta)=5\cdot\lambda_0$) θ=10° and mirrors are glass plates without coating ($R_1=R_2$=4.3 %). It is assumed in calculation that χ_0=0.3.

In Fig. 11 there is presented principal optical scheme of a LiF:F_2^- laser resonator with spectral selection: 1 is resonator mirror, mirrors 3, 4 and grating 7 form FPIG, 2 is FPI interferometer with short base for rough wavelength tuning, 5 is two optical wedges compensator for precise alignment of angle of incidence on grating, 6 is telescope with magnification 5^x – 10^x. Output radiation is showed by arrow. Precise tuning at the working wavelength can be done by rotating of the grating. But there is some technical problem. The tuning accuracy is about 0.1 cm^{-1}, so the accuracy of the angle of grating rotation should be about 10^{-5} rad (this follows from condition $\nu\sin(\theta)=\nu_0\sin(\theta_0)$=const.). This is small value and direct rotation of grating with this

accuracy is difficult to realise technically. Implementation of two optical wedges that are rotated around optical axis in opposite directions gives an easy and simple solution. Let us estimate feasibility of this compensator. Let it to be that in initial position two optical wedges are situated so that there is no deviation of propagation direction of light beam after passing through these wedges. If we rotate these wedges in opposite directions on angle 90 degrees then angle between input and output beams will be at maximum (or minimum). If angle of one glass wedge (refractive index 1.5) is 3' then rotation on 1 degree causes change of output beam angle about 10^{-5} rad. If one take into account that there is telescope with magnification $5^x - 10^x$ between optical compensator and grating (see Fig. 11) then it is clear that it is possible to ensure needed accuracy of laser radiation frequency tuning by this device.

Stable mode-locking regime of LiF:F_2^- laser (which is due to technical requirements to the laser) with resonator shown in Fig. 11 can be achieved if distance between mirrors 1 and 3 and distance between 3 and 7 are equal each other. If the grating has a capability of moving along the incident beam then these distances can be made equal each other. The possibility of displacement of grating should be taken into account in the laser construction.

For stable operation of the laser it is necessary to have some feedback to align the laser output radiation frequency. It can be done by different ways. One is implementation of external reference Fabry-Perot interferometer when deviation of frequency is converted into electrical signal proportional to frequency shift and this signal is used to monitor rotation of the optical wedges to change generation frequency. This feedback can ensure automatic control of a LiF:F_2^- laser frequency generation.

4. Continuous wave LiF:F_2^- - laser with narrow spectrum width.

The main idea of spectral selection described above was tested experimentally. LiF:F_2^- laser resonator scheme is presented in Fig. 12. Numbers from 1 to 8 denote the laser resonator parts, and 9 – 12 are parts of spectrum registration scheme. 1 is rear resonator mirror; transmission at 1.064 μm is 70%, reflectivity at 1.178 μm - 98%, radius of curvature 6.5 cm, 1.064 μm pump radiation is passing through this mirror; 2 is rotating LiF:F_2^- colour centres active element, length 28 mm, and weak field transmission at 1.064 μm 50%; 3 is lens with focal length 20 cm; 4 is flat mirror with reflectivity at 1.15 - 1.178 μm 66%. Parts 1 – 4 themselves form the additional LiF:F_2^- laser resonator. All experiments were done at pump power that exceeded threshold for this resonator. 5 is flat mirror with reflectivity at 1.15 - 1.178 μm 30%; 6, and 7 are lenses of telescope with magnification 5^x; 8 is grating with 300 grooves per mm. Distances are $L(1-2)$=5 cm, $L(1-3)$=33 cm, $L(1-4)$=110 cm, $L(4-5)$=24 cm, $L(4-6)$=40 cm, $L(4-7)$=88 cm, $L(4-$

9)=91 cm. We made 1 – 4 resonator length shorter than in previous case (see Fig. 4) because mechanical stability for this resonator was higher. Parts of spectrum registration scheme are 9 – Fabry-Perot illuminating lens f=5 cm; 10 - Fabry-Perot interferometer with base 8 mm; 11 – objective with focal length f=16 cm; 12 – CCD – camera.

It was tested experimentally that spectrum of radiation that is passed through mirror 4 and reflected by mirror 5 is the same as in the direction showed by arrow. In the last case registration is easier to do because there is no interference from pump radiation. And one more remark concerning the experiment. For efficient spectral selection it is important to align distance between lenses of telescope 6 and 7 to have flat wave front of radiation incident on the grating 8.

In Fig. 13 there is spectrum of cw LiF:F_2^- laser radiation. Estimated from Fig. 13 *b* spectrum width is less than 0.1 cm^{-1}. Stability of radiation frequency was better than the estimated spectrum width during 20 minutes of laser work. Weak additional peak in Fig. 13 *b* is probably due to a reflection from some internal resonator element because its intensity depends on resonator alignment. Output power and exact wavelength of generation were not measured.

5. Future Directions

Let us enumerate here the ways to improve the LiF:F_2^- laser performance.

1. Perfection of the spectral selection scheme.

1.1. Optimisation of its mirrors reflectivity from the point of view the laser efficiency and spectral selectivity;

1.2. Experimental determination of parameters spectral selection elements (telescope, grating, and optical wedges) to have needed spectral purity of the laser radiation;

1.3. Development of electronic and optical parts of the scheme to monitor wavelength of radiation;

1.4. Development of stable mechanical construction of the laser.

2. Rising of output power of the LiF:F_2^- laser. To have higher output power in our laser the only is necessary to rise pump power. Estimations show that there are no principal limits from the point of view heat removing from rotating LiF active element at least up to 1 kW of heat power dissipating in the crystal. The only is necessary to choose appropriate dimensions of LiF and rotation speed.

It is possible to use experimental data presented in Fig. 6 to evaluate output power of LiF:F_2^- laser at high pump power. In Fig. 14 there is estimation dependence of output power as function pump power of cw LiF:F_2^- laser at conditions of the experiment (see Fig. 6) except for output

mirror reflectivity which is assumed 30%. From Fig. 14 one can see that at pump power 200 W it is possible to expect output power about 50 W.

3. Implementation of laser diodes as pump source for the LiF:F_2^- laser. Choosing of pumping radiation wavelength at peak of absorption F_2^- cc gives the possibility to have length of the LiF crystal smaller at the same concentration of the cc, and to have lower level of passive losses at wavelength of generation which in turn leads to higher efficiency of laser generation.

6. Conclusion

Construction of rotating LiF active element was developed. Mechanical parts of the construction were manufactured and device was put into operation.

Continuos wave operation of a LiF: F_2^- laser with rotating active element was obtained. Output power was 270 mW at pump power 9 W. Wavelength of generation was 1.15 μm.

Spectral characteristics of a Fabry-Perot interferometer with grating as one of its mirror were discussed. Results of calculation were presented for particular parameters of the interferometer.

It was suggested to use Fabry-Perot interferometer with grating as output mirror of a tuned LiF:F_2^- laser. The main advantage of the interferometer is a possibility to implement it in the lasers with low gain that are sensitive to internal resonator losses. At the same time spectral selectivity of the interferometer can be made as good as it is necessary to meet the requirements to spectral purity.

The scheme of a LiF:F_2^- laser with special parameters of reflection coefficients of mirrors and grating was suggested.

The problem of fine frequency tuning was discussed and it was suggested to use two optical wedges for this purpose.

Suggested scheme of spectral selection was realised experimentally. It was obtained spectral width of radiation less than 0.1 cm^{-1}. Frequency stability of radiation was better than 0.1 cm^{-1} during 20 minutes of work. This experimental data show that the scheme of spectral selection is workable in principal.

Some questions that are concerned with further improvement of LiF:F_2^- laser performance are enumerated. Among them are spectral selection and output radiation frequency monitoring, high output power, and pumping with laser diodes.

References

1. Contract F61708-97-W0127 Laser with Wavelength 0.589 μm ("Sodium Wavelength Laser"). Final report (1998).

2. Laser with Wavelength 0.589 μm ("Sodium Wavelength Laser"). Contract F61775-98-WE057. Final report. (1999).

3. Yu.L.Gusev and S.N.Konoplin. Kvant. Elektron., v.8 #6, 1343 (1981). [Sov. J. Quantum Electron. v.11, #6, 808 (1981)].

4. M. Born, E. Wolf. Principles of Optics. Pergamon Press, 1964.

5. R.W.Ditchburn. Light. Blackie&Son Ltd. 1959.

6. S.P.Anokhov, T.Ya.Marusiy, M.S.Soskin. Tuned Lasers, Moscow, Radio and Svayz, 1982. (in Russian)

7. S.M.Kopilov, B.G.Lisoi, S.L.Seregin, O.B.Cherednichenco. Tuned Dye Lasers and Applications. Moscow, Radio and Svayz, 1991. (in Russian)

8. T.T.Basiev, P.G.Zverev, A.G.Papashvili, V.V.Fedorov. Kvant. Elektron., v.24, #7, 591 (1997). [Sov. J. Quantum Electron. v.27, #7, 574 (1997)].

Principal Investigator Nikolay Ilichev

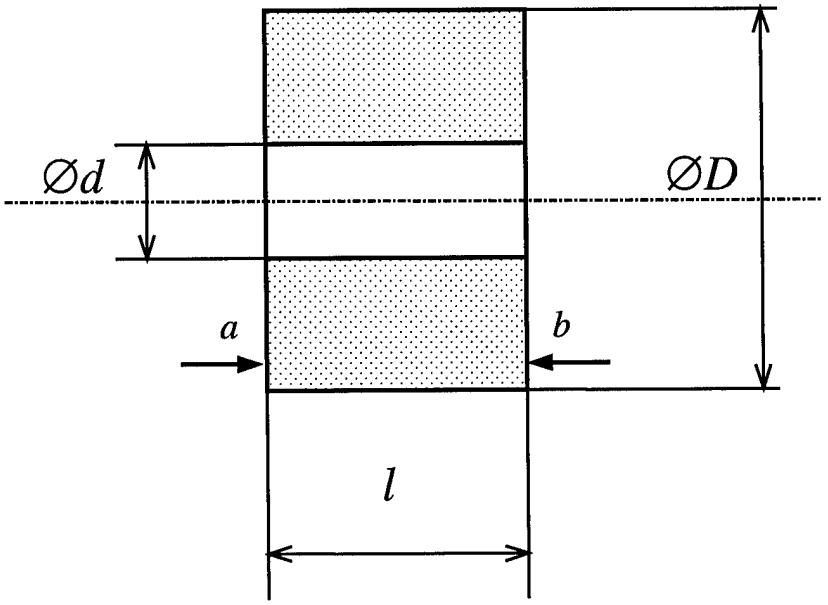

Fig. 1. Draft of LiF crystal active element. Dimensions: $\varnothing d$=15 (±0.2) mm, $\varnothing D$=50 (±0.2) mm, l=28 mm.

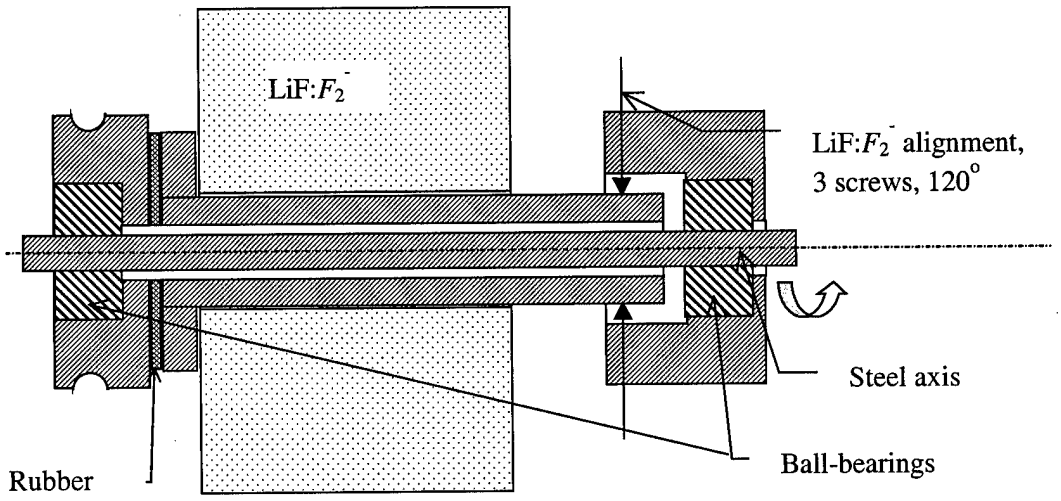

Fig. 2. Layout of LiF rotation scheme. Steel axis is resting and all other parts are rotating in ball-bearings.

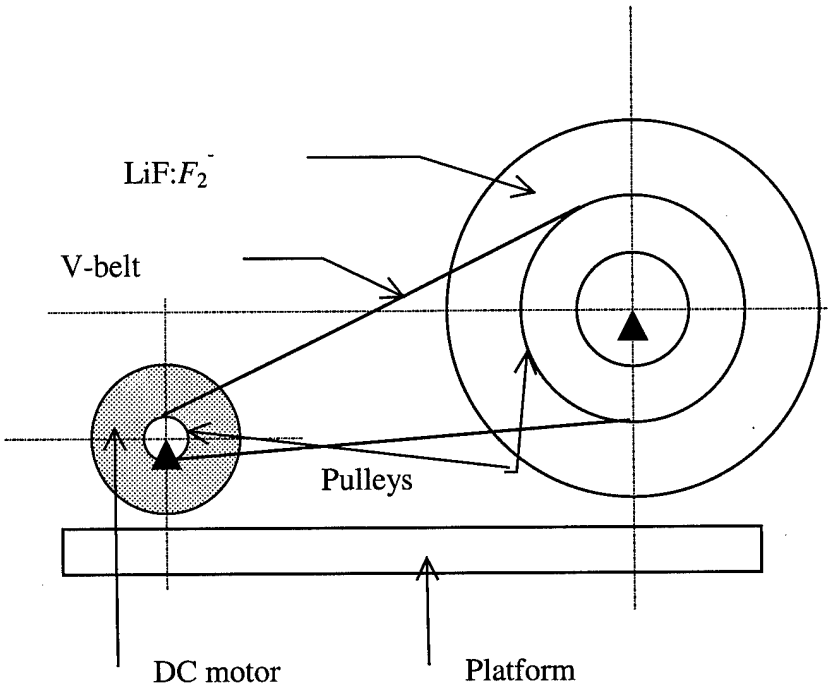

Fig. 3. Kinematic scheme of LiF rotation.

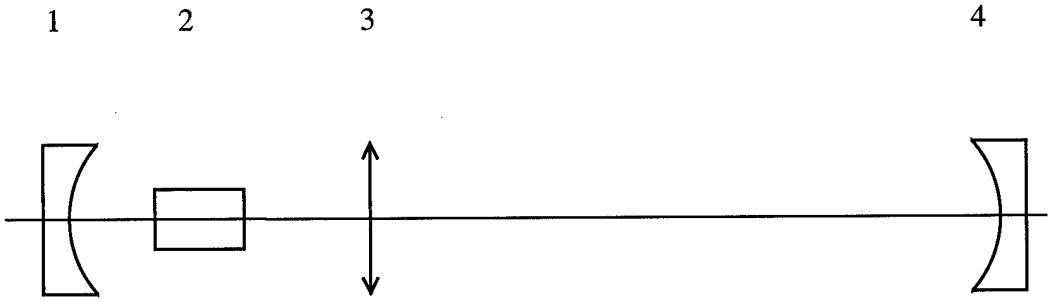

Fig. 4. Layout of LiF:F_2^- laser resonator.

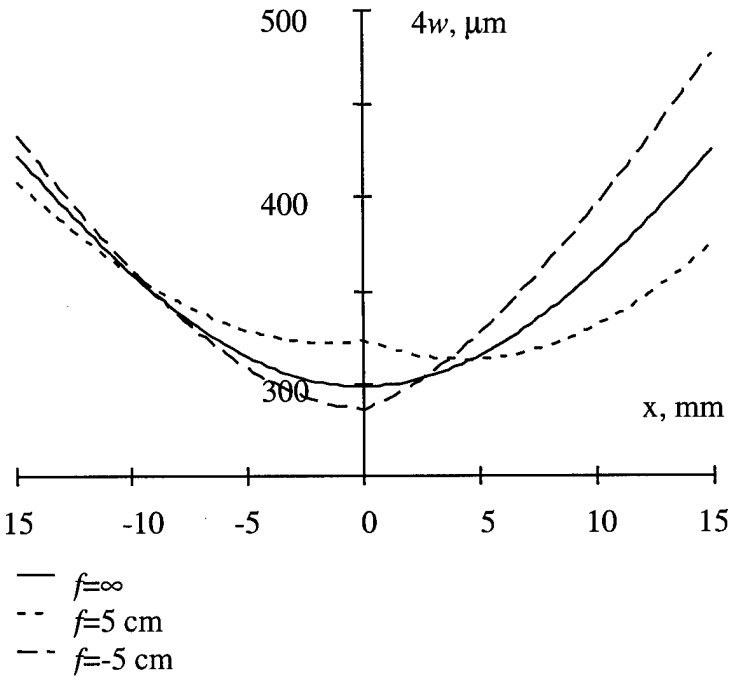

Fig. 5. TEM_{00} – mode diameter ($4w$) as function of co-ordinate along optical axis from middle of active element for three values of focal lengths of thermal lens. Intensity of the TEM_{00} mode is $\exp(-2(r/w)^2)$.

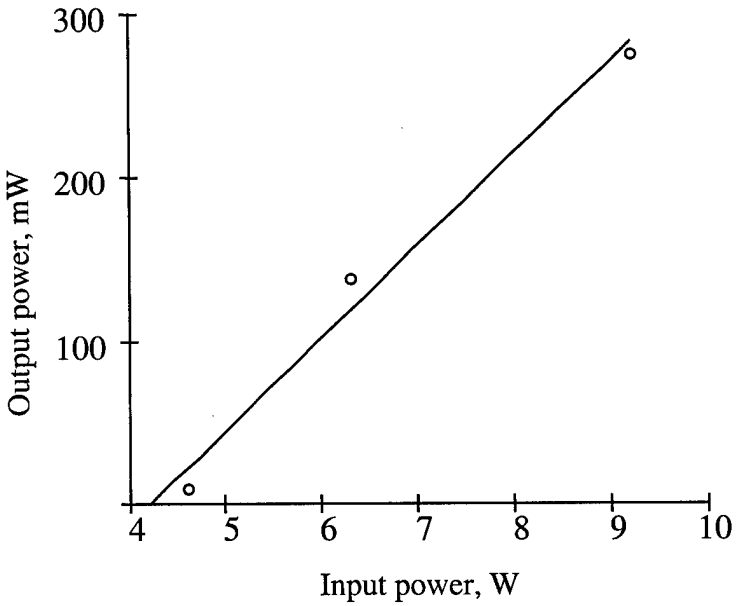

Fig. 6. Output power of LiF:F_2^- - laser as function of input power; circles are experimental points.

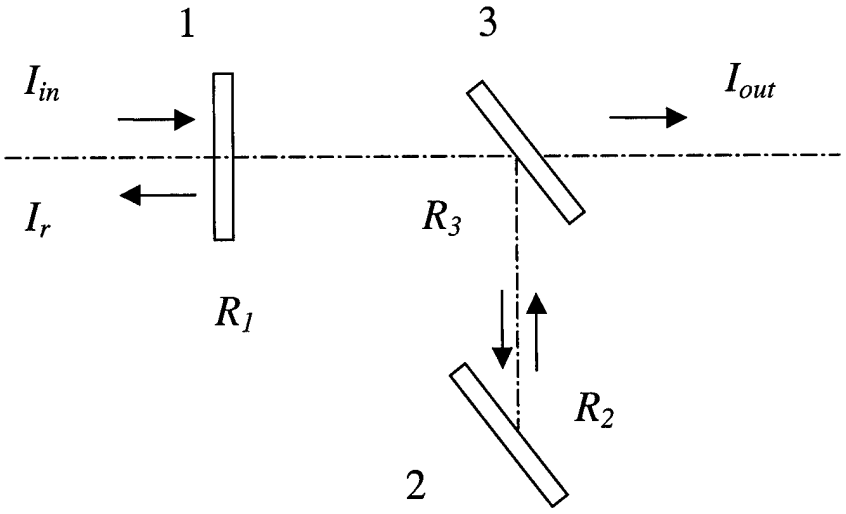

Fig. 7. Scheme of Fabry-Perot interferometer with grating.

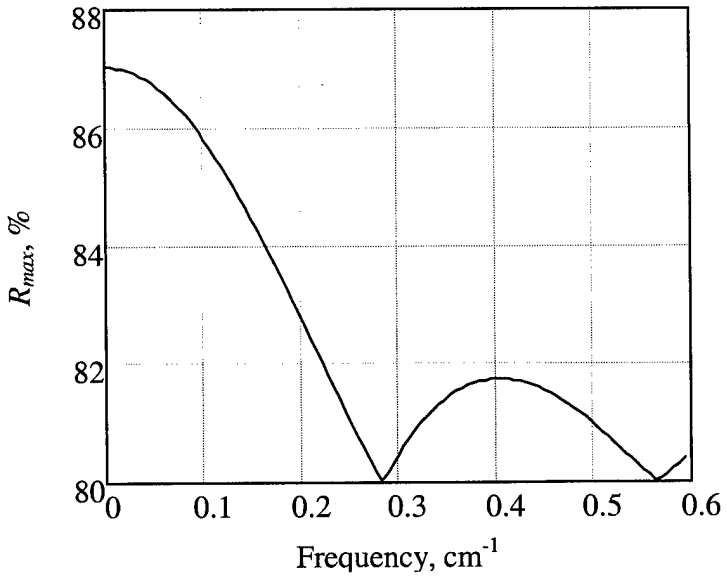

Fig. 8. Reflectivity coefficient of FPIG as function of frequency ν-ν_0 at maximum.

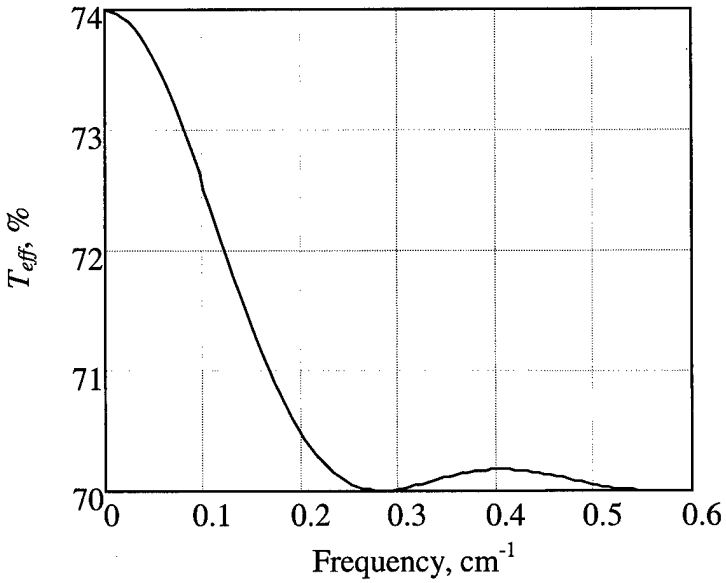

Fig. 9. Effective transmission as function of deviation of frequency ν-ν_0.

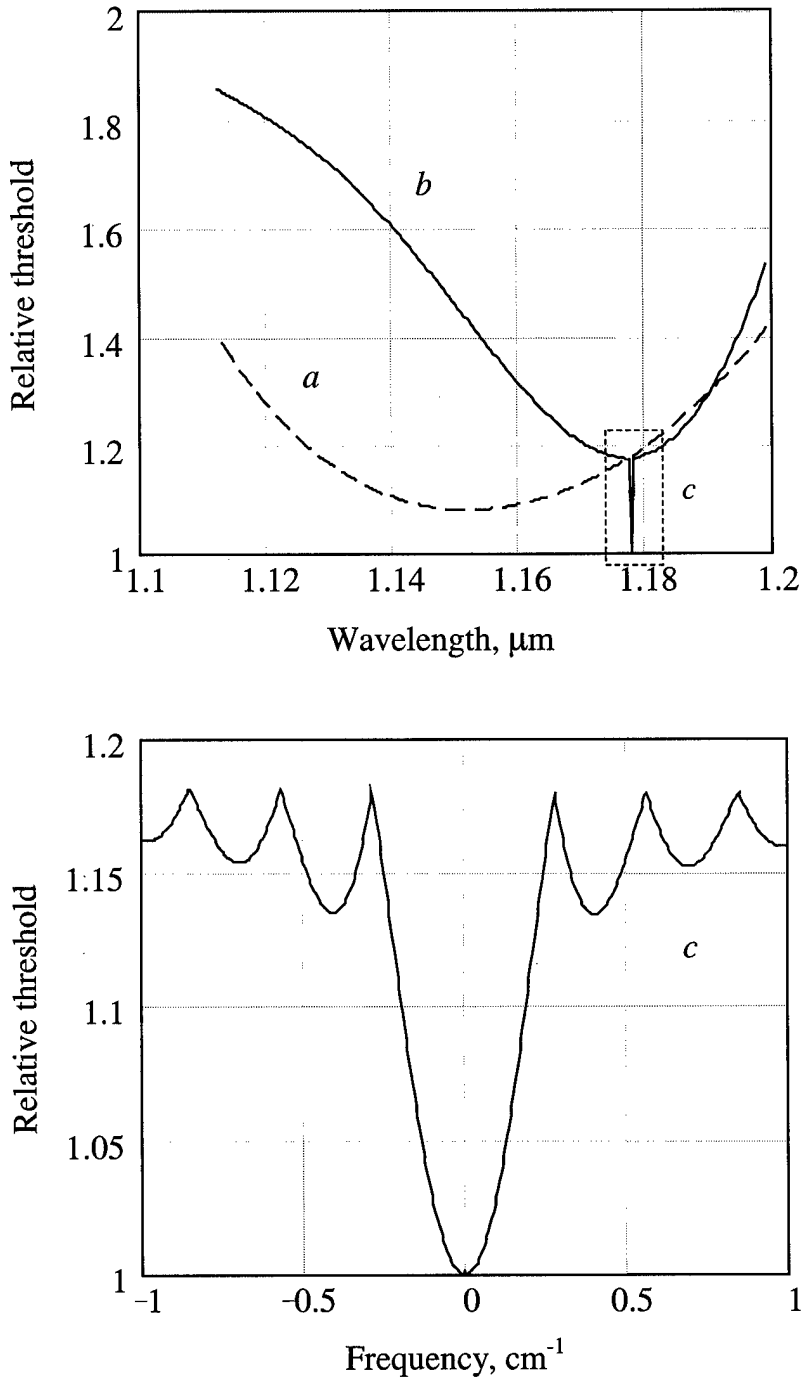

Fig. 10. Relative threshold $\gamma(\nu)$ as function wavelength: *a* – without interferometer Fabry-Perot in a LiF:F_2^- laser resonator, *b* – with Fabry-Perot interferometer in the resonator, and *c* – part of curve *b* as function of deviation of frequency ν-ν_0 in the vicinity of ν_0.

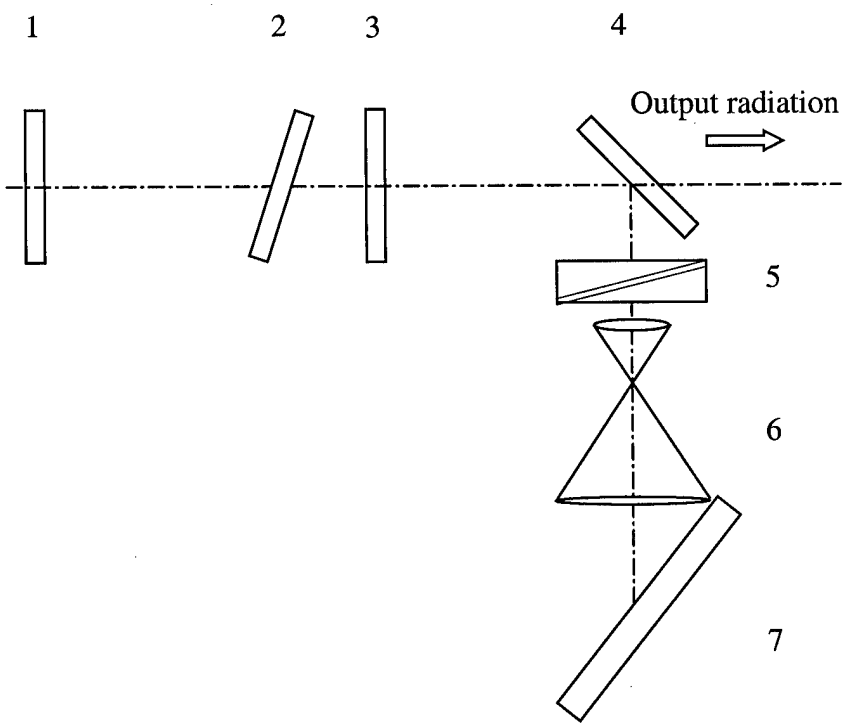

Fig. 11. Principal optical scheme of a LiF:F_2^- laser resonator with spectral selection.

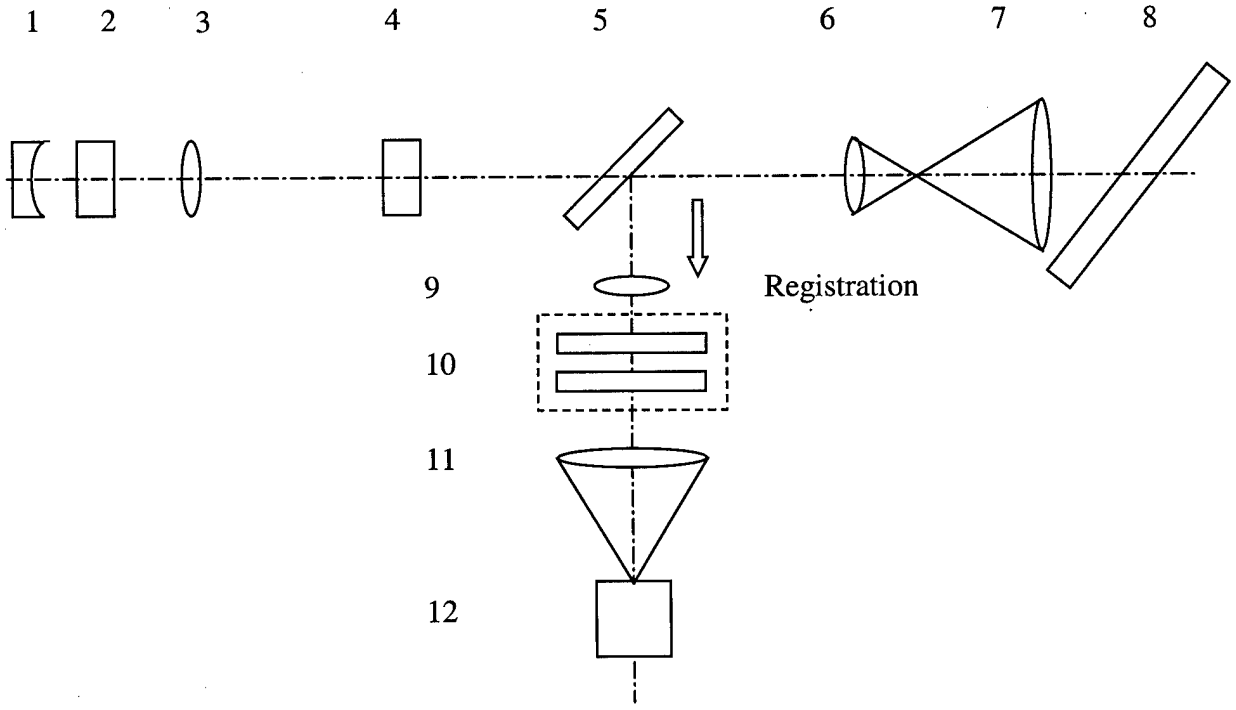

Fig. 12. Scheme of LiF:F_2^- cc laser with narrow spectrum width.

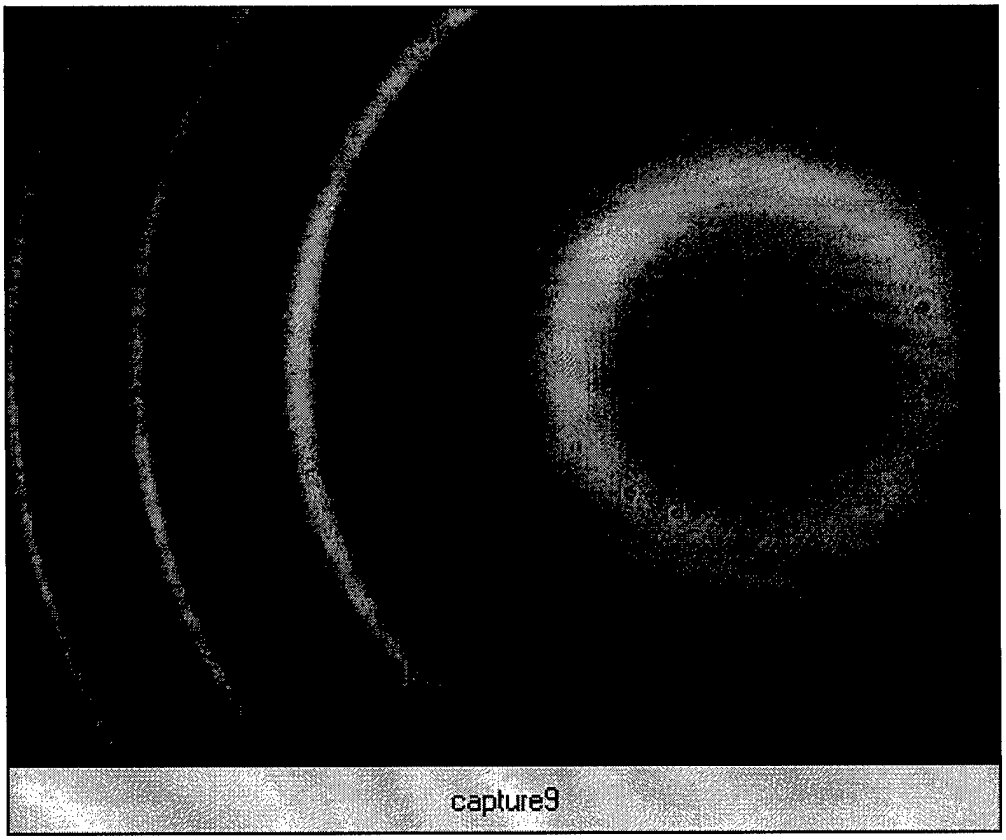

a

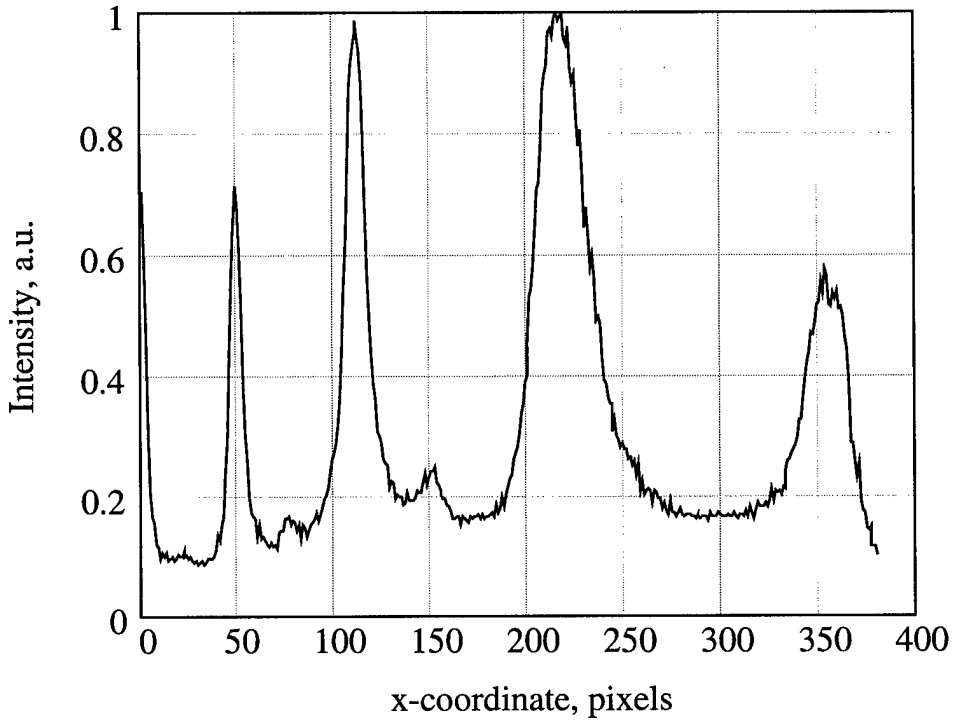

b

Fig. 13. Fabry-Perot interferogram of cw LiF:F_2^- laser radiation: *a* – rings picture, *b* - intensity distribution, scanning is in x direction; strip scanning y width of is 11 pixels. Fabry-Perot base is 8 mm; spectrum width is less than 0.1 cm^{-1}.

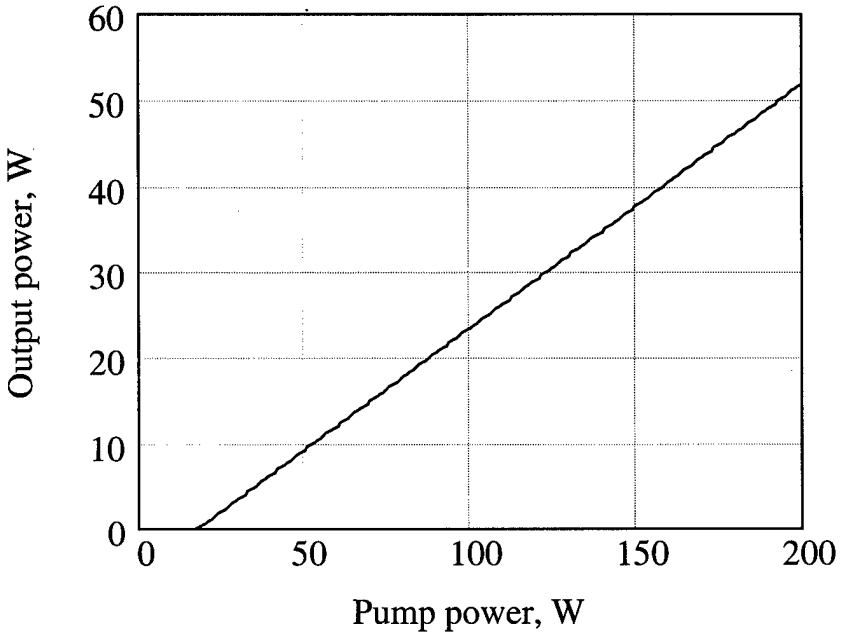

Fig. 14. Evaluation curve of output power as function of input power for a LiF:F_2^- laser. Reflectivity of output mirror is assumed 30%.